Effect of graphene oxide sheet size on the curing kinetics and thermal stability of epoxy resins

Xiao Wang[1], Jie Jin[2], Mo Song[2] and Yue Lin[3]

[1] Center of Membrane Technology and Application Engineering, Chongqing Institute of Green and Intelligent Technology, Chinese Academy of Sciences, Chongqing 400714, China.

[2] Department of Materials, Loughborough University, Loughborough, Leicestershire LE11 3TU, UK

[3] School of Materials, University of Manchester, Oxford Road, Manchester M13 9PL, UK

E-mail: wangxiao@cigit.ac.cn

Keywords: graphene oxide, epoxy resin, curing kinetics, thermal stability, sheet size

Abstract

This work revealed the influences of graphene oxide (GO) sheet size on the curing kinetics and thermal stability of epoxy resins. A series of GO/epoxy nanocomposites were prepared by the incorporation of three different sized GO sheets, namely GO-1, GO-2 and GO-3, the average size of which was 10.79μm, 1.72μm and 0.70μm, respectively. The morphologies of the nanocomposites were observed by field emission gun scanning electron microscope (FEGSEM). The dispersion quality of each sized GO was comparable in the epoxy matrix. The curing kinetics was investigated by means of differential scanning calorimetry (DSC) and analysed based on kinetics model. Addition of a small amount of GO (0.1 wt%) exhibited strong catalytic effect on the curing reaction of epoxy resin. The activation energy was reduced by 18.9%, 28.8% and 14.6% with addition of GO-1, GO-2 and GO-3, respectively. GO-2 with medium size (1.72μm) showed the most effective catalysis on the cure. The thermal stability of the cured resins was evaluated based on thermogravimetric analysis. GO/epoxy nanocomposites showed improved the thermal stability in the range of 420-500 ^{o}C, compared with the pure resin. A ～4% more residue was obtained in each of the incorporated system. The variations of GO sheet size did not influence the enhancement effect on the thermal stability.

1. Introduction

Epoxy resins, which possess low cost and health hazard, have been the most important thermosetting resins in industry for various applications. They have been widely used as engineering adhesives, paints, surface coatings, electrical insulations, construction materials and components for automotive, marine and aerospace composites [1]. Recently, reinforcements of epoxy resins by the addition of nanofillers have been intensively reported [2–5]. The epoxy nanocomposites show improved properties with a low filler loading. The nanoparticles are more efficient in enhancing the performances of epoxy resins, compared with traditional particles. It has been demonstrated that the properties of epoxy and its nanocomposites highly depend on the effects of nanofillers on the curing behavior of the matrix [6–9]. They could catalyze the curing process and influence the network formation of the resin. On the contrary, the nanofillers could act as physical hindrance that inhibits the cure of chains. These effects could change the curing kinetics, network formation and structure of the composite, and finally affect its properties. Therefore, in order to develop high performance epoxy nanocomposite, it is essential to understand how the addition of nanofillers influences cuing kinetics.

Epoxy resins are oxirane-containing oligomers that require suitable hardener to participate the reaction of epoxide groups. The cure of epoxy resins shows auto-catalyze behavior caused by the –OH groups generated during the cure [10]. For a diglycidyl ether of bisphenol-A (DGEBA)/ 4,4'-diaminodiphenylsulfone (DDS) system, in the course of cure, each primary amine of DDS reacts with an epoxy group of DGEBA, via ring opening, and forms a CH_2-NH bond as well as a pendant hydroxyl group. The hydroxyl group is known to accelerate subsequent ring opening reactions. The resultant secondary amines further react with remaining epoxy rings in a similar manner, by which the polymer chains are crosslinked at a slower rate [11]. Accordingly, the nanofillers with functionalized groups such as hydroxyl could affect the curing behavior of epoxy resins. So far, the influences of various nanofillers have been investigated and reported. Zhang et al. [12] found that the incorporation of POSS-NH_2 decreased the reaction rate of epoxy resins at early stages, while this effect was not obvious at the late stages of the curing reaction. The average activation energy of the curing reaction of the epoxy nanocomposites was higher than the pristine system. In contrast, the presence of nanosilica was reported to act as catalyst that led to a higher reactivity and decreased the activation energy of epoxy resins [13]. Ferdosian et al. evaluated the catalytic effect of nanoclay on the epoxy resins. The addition of clay reduced the activation energy of the cure reaction [14]. Similar catalytic behavior in the curing process of epoxy nanocomposites was also observed by the incorporation of carbon nanofillers such as CNTs [15, 16], carboxylic functionalization of CNTs [17, 18], silica-coated CNTs [19] and carbon black [6]. However, carbon nanofibres (CNFs) [20, 21] or fluorine modified CNTs [22] hardly affected the cure kinetics of epoxy resins. Expanded graphite (EG) did not significantly impede the cure of epoxy [23], and its effect was related to the concentration of EG incorporated [24].

Among the nanoparticles, graphene is a two dimensional materials with high aspect ratio and tremendous surface area. Its advantages in reinforcing epoxy resins over other fillers have been reported [25, 26]. However, the performances are highly dependent on the size of graphene incorporated. Recent work has revealed that the sheet size of graphene oxide (GO) significantly influences the fracture toughness [25] and the mechanical properties [27] of GO/epoxy nanocomposites. In the investigations of the effect of GO on curing behavior of epoxy resins, Qiu at al. [28] found that the presence of GO slightly decreased the curing temperature of epoxy resins. The oxygen functionalities including hydroxyl and carboxyl groups on the GO catalyzed the curing reaction. Activation energy of the reaction reduced with the increase of GO content, especially in the later stage. However, it conflicts with Ryu [29] and Li's [30] study, where the activation energy increased by the addition of GO in the epoxy resins. The effect of GO on the curing process of epoxy is still in debate. On the other hand, in order to meet the demand for high temperature applications of epoxy resins, it is important to investigate the thermal stability of the epoxy and its nanocomposites with GO. Although a few studies have been done to evaluate their thermal properties [31–33] and the curing behavior, the effects of GO sheet size are not clear. In this study, three different sized GO sheets were used to prepare a series of GO/epoxy nanocomposites. We attempt to reveal the effects of GO sheet size on the curing kinetics and thermal stability of epoxy resins. This work essentially contributes to a judicious selection of filler size in the development of epoxy nanocomposites.

2. Experimental

2.1. Materials

Three sizes of graphite flakes, which were denoted as G-1, G-2 and G-3, were purchased from Qingdao Graphite Company. The average size of the graphite flakes was 150μm, 7μm and 4μm, respectively. Diglycidyl ether of bisphenol-A (DGEBA) epoxy (D.E.R*331) (epoxide equivalent weight is 182–192 g•eq^{-1}) was obtained from Dow Chemical. The 4,4'-diaminodiphenylsulfone (DDS) curing agent was supplied by Sigma-Aldrich. Their structures were presented in figure 1. Acetone was provided by Fisher-Scientific Ltd.

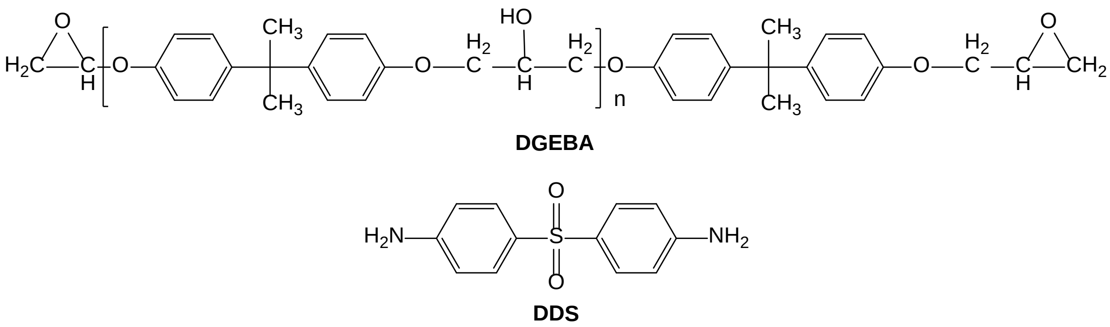

Figure 1. Structures of DGEBA and DDS.

2.2. Fabrication of GO and GO/epoxy mixture

GO was fabricated from graphite by using Hummers' method [34]. The GO was denoted as GO-1, GO-2 and GO-3, respectively. In terms of the preparation of GO/epoxy mixture, the GO was firstly dispersed in acetone at concentration of 1 mg ml^{-1}, by means of ultrasonication for 30 min (300 w) at room temperature. DGEBA/GO mixtures were then prepared by adding calculated amount of GO (0.1 wt%) into the DGEBA. The mixture was stirred at 80^{o}C for 1 h, followed by degassing in a vacuum oven (800 mBar) for 1 day at 80^{o}C to remove the solvent.

DDS curing agent was added into the DGEBA/GO mixture and stirred at 135°C for 1 h. The weight ratio of DDS to DGEBA was 1:4. All the prepared GO/epoxy mixtures were sealed and stored at -20°C for further use.

2.3. Characterization

A Shimadzu Fourier Transform Infrared (FTIR) 8400s spectrophotometer was used to record the spectra of the three types of GO in the range of 4000 to 750 cm^{-1}. The resolution is 2 cm^{-1} over 64 scans. Particle size of GO was determined by using a Malvern Instruments Mastersizer. Layered GO structure was observed by a Philips Tecnai high resolution transmission electron microscopy (HRTEM). The GO was dispersed in acetone, and dropped on copper grid for observation. A TA Instruments Differential Scanning Calorimetry (DSC) calorimeter was used for quasi-isothermal tests, in order to reveal the curing behavior of epoxy and its nanocomposites at 170°C, 175 °C and 180 °C, respectively. All the tests were run under a modulated-temperature DSC model with modulation amplitude of 0.5 °C and a period of 60s. Nitrogen gas rate was 60 ml min^{-1}. A field emission gun scanning electron microscope (FEGSEM) LEO 1530VP was used to observe the cross-sectional morphology of the fully cured epoxy and its nanocomposites. The samples were prepared by curing the mixtures at 180°C for 1 h, 200°C for 2 h and post-cured at 250°C for 2 h. Before observation, the cured samples were freeze-fractured in liquid nitrogen and coated with gold by a sputter coater for 60s. The images were taken from area with minimal number of cracks, in order to get good observation of GO dispersion. The thermal stability of the cured epoxy resin and the nanocomposites was revealed by means of thermogravimetric analysis (TGA) on a DSC-TGA 2950 instrument. The samples were heated from 50°C to 700 °C at a rate of 10 °C min^{-1}. The air rate was 50 ml min^{-1}.

3. Results and discussion

Figure 2 shows the FTIR spectra of the three types of GO. They exhibited comparable spectra with the characteristic bands observed at 1250 cm^{-1} (C-O-C), 1745 cm^{-1} (C=O) and 3420 cm^{-1}

(-OH). It indicates that the three types of GO were functionalized with epoxide, carboxyl and hydroxyl groups, by means of the Hummers' method. Particle size distribution of the three types of GO was measured and shown in figure 3. Table 1 lists the typical size parameters, including D_{20}, D_{50} and D_{80}, which represented the particle size at which 20%, 50% and 80% of the GO sheets was below this given size. It can be noticed that the GO sheet size decreased from GO-1 to GO-3. In particular, the average size, D_{50}, of GO sheets for GO-1, GO-2 and GO-3 was 10.79μm, 1.72μm and 0.70μm, respectively. The edges of the GO sheets were observed by means of HRTEM technique, in order to reveal the layered graphene platelet structure. Based upon a sufficient quantity of observations on the GO sheets, for each type of GO sheets, they were comprised with about 2-5 individual graphene layers. The thickness of the GO sheets was about 1-2 nm. Figure 4 shows the typical images of the edges for GO-1, GO-2 and GO-3. According to the FTIR analysis, size distribution measurement and HRTEM microscopy, the three types of synthesized GO had similar surface chemistry and thickness but differed in surface size. The SEM cross-sectional images of the dispersion morphology for the epoxy and its nanocomposites with the three different sizes of GO were shown in figure 5. It can be observed that the GO sheets were well dispersed in the epoxy matrix. The dispersion quality of each type of GO was comparable. The sizes of the GO sheets were unchanged in the composites. The preparation process did not affect the original sheet size of GO.

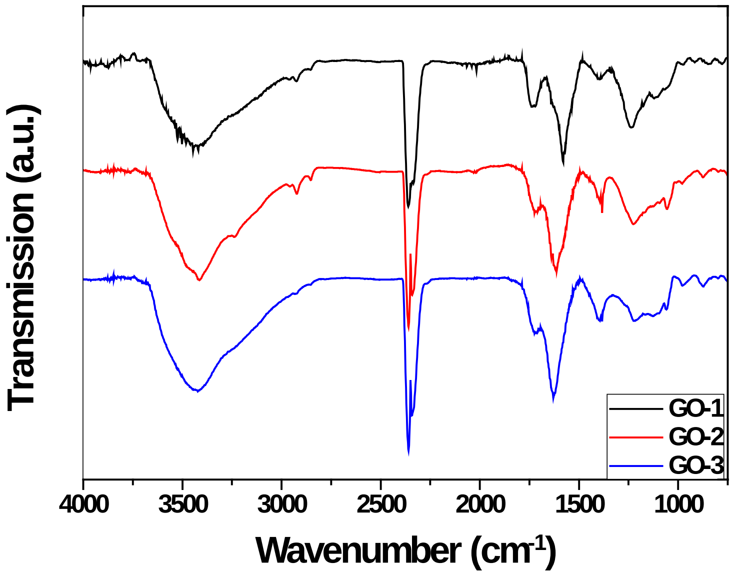

Figure 2. FTIR spectra of GO-1, GO-2 and GO-3. The spectra were parallel shifted for clarification.

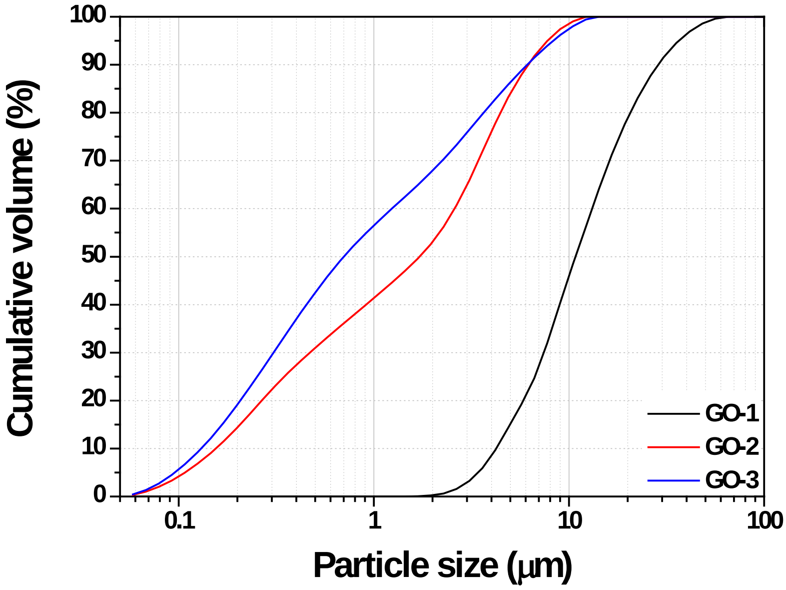

Figure 3. Particle size distribution of GO-1, GO-2 and GO-3.

Table 1. Key parameters of GO sheet size.

Type	GO-1	GO-2	GO-3
D_{20}(μm)[a]	5.82	0.27	0.21
D_{50}(μm)[a]	10.79	1.72	0.70
D_{80}(μm)[a]	20.71	4.48	3.66

[a] D_{20}, D_{50} and D_{80} represent particle size at which 20%, 50% and 80% of the GO is below this given size, respectively.

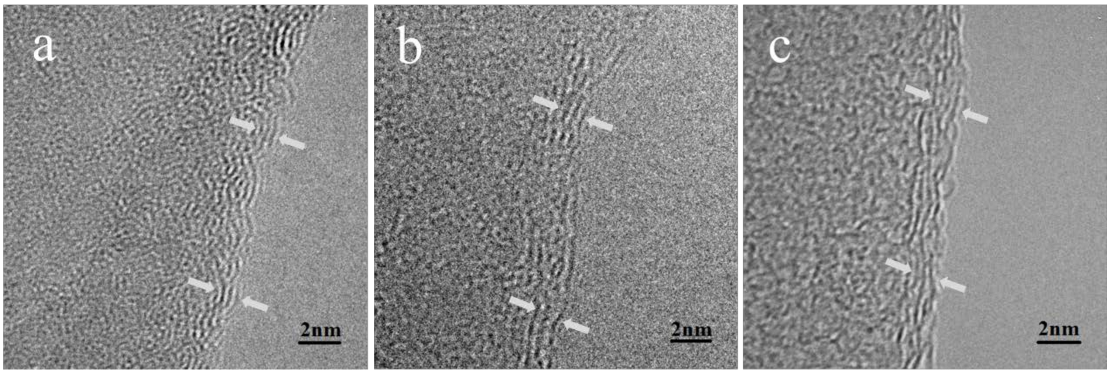

Figure 4. HRTEM images of the edges of (a) GO-1, (b) GO-2 and (c) GO-3, showing the layered structure. The thickness of the GO sheets was about 1-2 nm.

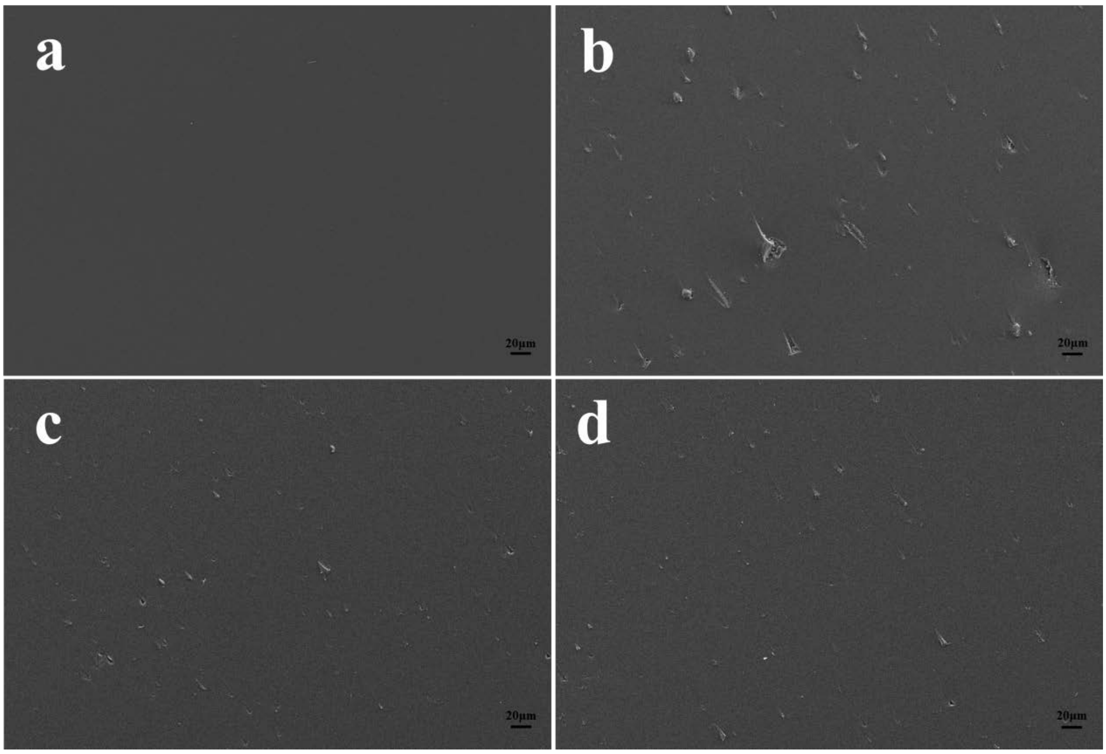

Figure 5. SEM cross-sectional images of morphologies for (a) epoxy and its nanocomposites with 0.1 wt% (b) GO-1, (c) GO-2 and (d) GO-3.

The curing kinetics of epoxy nanocomposites is vitally important. It reveals the curing course including conversion, reaction rate and activation energy. They highly influence the processing ability, network structure and properties of the nanocomposites [32]. The key curing kinetics parameters were assessed by means of quasi-isothermal DSC analysis.

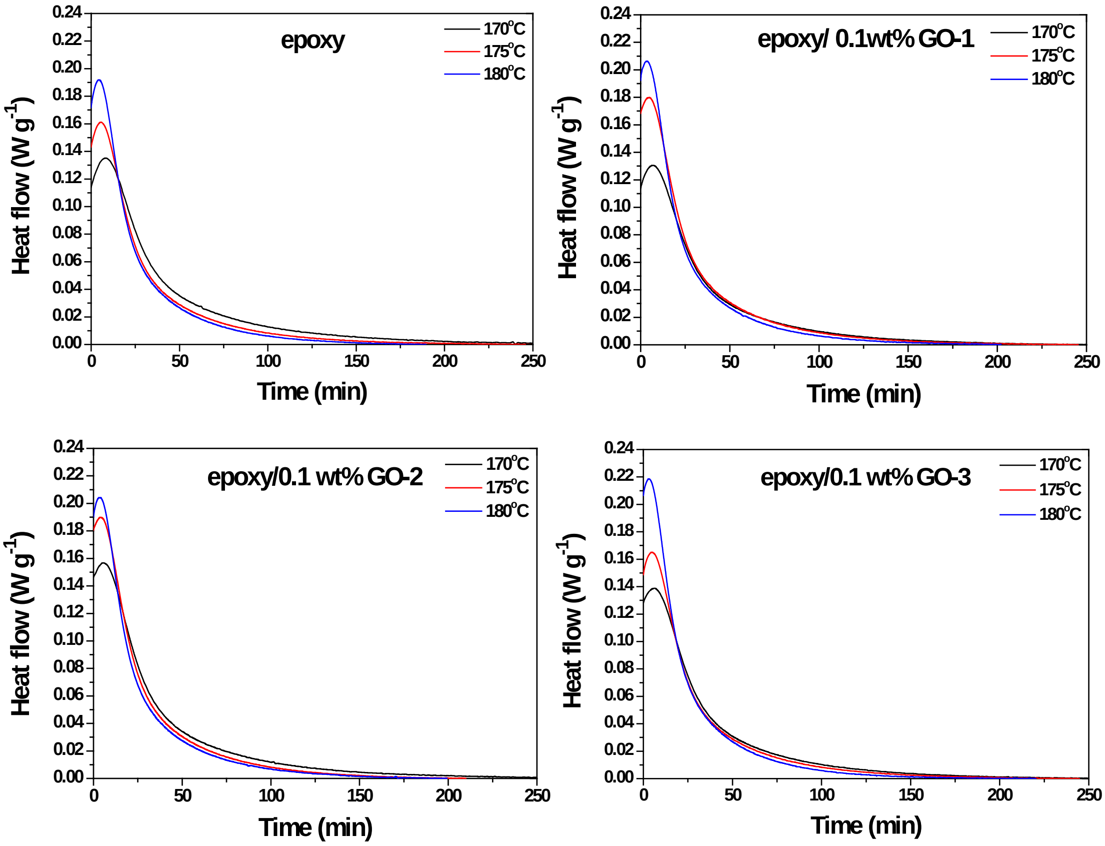

Figure 6. Isothermal DSC plots of the GO/epoxy nanocomposites at different curing temperatures.

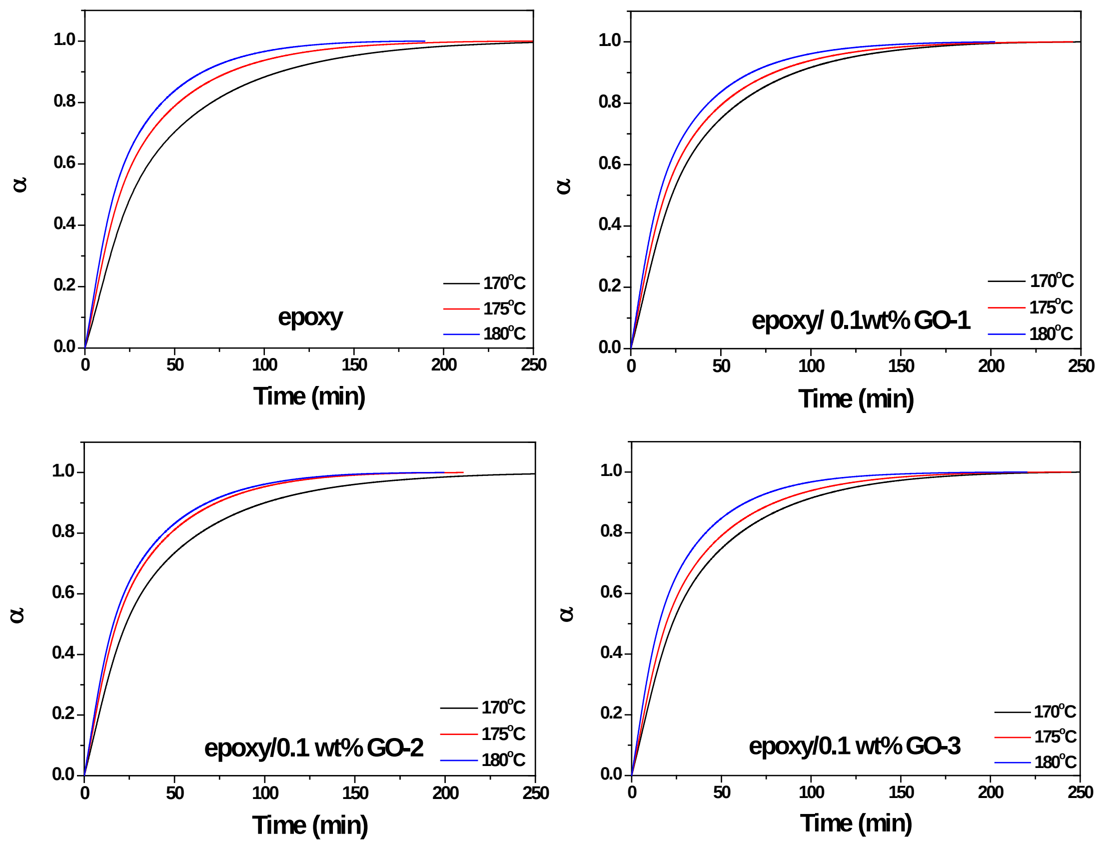

Figure 7. Conversion, *α*, versus curing time for the GO/epoxy nanocomposites at different curing temperatures.

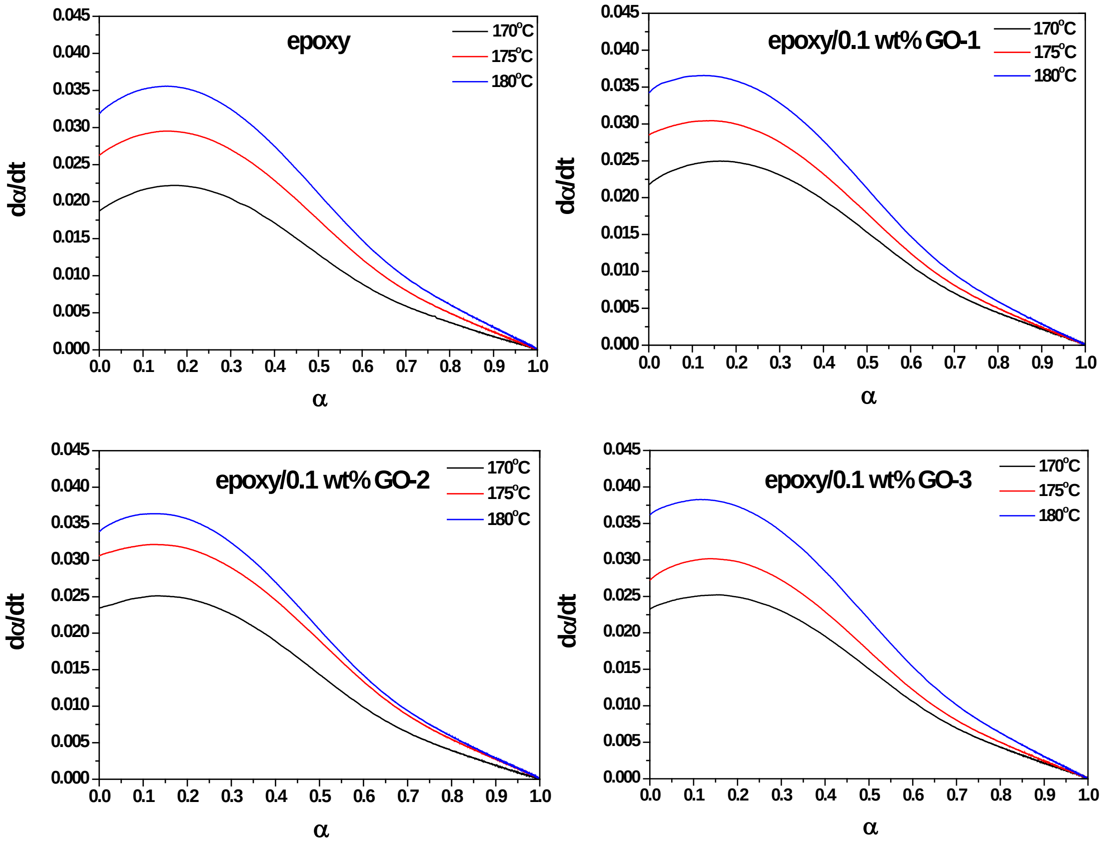

Figure 8. $d\alpha/dt$ versus α for the GO/epoxy nanocomposites at different curing temperatures.

Table 2. Comparison of curing parameters for epoxy and its nanocomposites at different curing temperatures.

Temperature (°C)	Epoxy	GO-1/epoxy	GO-2/epoxy	GO-3/epoxy
	Time (min), when maximal heat flow is observed			
170	8.18	6.90	5.39	6.25
175	5.37	4.80	3.96	4.68
180	4.47	3.52	3.50	3.08
	α', conversion where maximal $d\alpha/dt$ is observed			
170	0.177	0.161	0.127	0.154
175	0.154	0.139	0.125	0.141
180	0.150	0.126	0.120	0.113

Figure 6 shows the isothermal DSC plots of heat flow versus curing time for the epoxy resin and its nanocomposites with three types of GO at different curing temperatures. The commencement of curing reaction was accompanied by high value of heat flow, revealing fast initiation process of DGEBA and DDS molecules. Oligomers were subsequently formed and the chains were built up linearly, where the molecular weight continuously increased. Maximal heat flow was observed a few minutes after the start of reaction. As the curing reaction further proceeded, the polymer chains were crosslinked, followed by the formation of three-dimensional network. The reaction heat flow decreased and finally approached down to zero, suggesting the end of the cure. The GO/epoxy nanocomposites exhibited similar variation of heat flow versus time. However, the maximal heat flow was appeared earlier than pristine epoxy. The corresponding time was referred and listed in table 2. The presence of GO could accelerate the curing reaction of epoxy resin. Figure 7 shows the plots of conversion, α versus time for epoxy and its nanocomposites. α represents the degree of reaction at the particular temperature.

$$\alpha = \frac{\Delta H_t}{\Delta H_T} \quad (1)$$

where ΔH_t is the reaction heat from the onset of polymerisation up to time, t, ΔH_T is the total reaction heat at the particular curing temperature. The residual reaction heat was not considered in this study, as it related to the post-cure course. $d\alpha/dt$ is defined as conversion rate at time, t.

$$\frac{d\alpha}{dt} = \frac{1}{\Delta H_T}\frac{d\Delta H_t}{dt} \quad (2)$$

The plots of $d\alpha/dt$ versus α are shown in figure 8. It can be observed that during the initiation stage of the curing, the conversion rate of pure epoxy resin increased with the curing process. The reaction intermediates were formed and increased to a sufficient amount, auto-accelerating the reaction. A maximal conversion rate appeared between α = 0.150-0.177. At higher conversion, the reaction rate decreased owing to the increased viscosity. The trend of the conversion rate was in agreement with auto-acceleration behaviour. With the incorporation of GO, the conversion at the maximal conversion rate (this particular conversion is defined as α') was shifted to lower value, as demonstrated in table 2. In general, the shift of α' reveals a catalytic effect of a filler on cuing reaction [7]. Thus, in this study, the GO could catalyze initial stage of epoxy curing. The catalyzed stage then induced a fast generation of reaction intermediates, followed by an earlier appearance of the maximal conversion rate, compared with pure resin.

The cure of the GO/epoxy system included several competing reactions. The main mechanism of the catalytic effect of GO on the epoxy curing was illustrated in figure 9. It involved addition and etherification reactions. As presented in figure 9a, Carboxyl (or hydroxyl) group of GO enabled the formation of hydrogen bond with DGEBA, followed by a GO-DGEBA-DDS trimolecular transition complex. The complex was able to accelerate epoxide ring opening. Subsequently, Secondary amine was formed after fast proton transfer. The resultant secondary amine could further react with remaining DGEBA in a similar manner, by the presence of GO catalyst (figure 9b). The epoxide rings were consumed rapidly. When the concentration of unreacted epoxide rings approached to a very low level, GO reacted with the pendant hydroxyl group, creating ether link after dehydration (figure 9c).

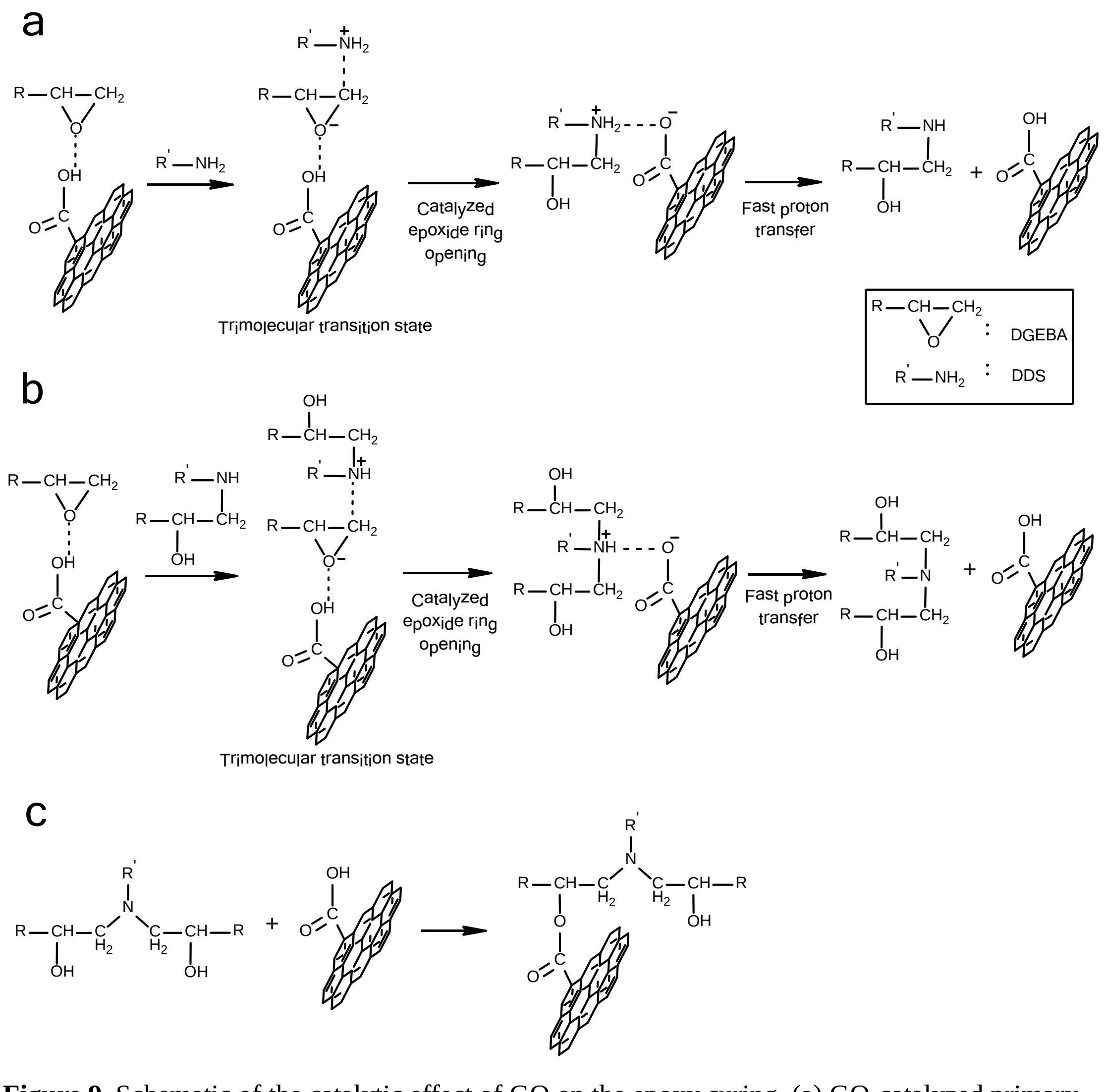

Figure 9. Schematic of the catalytic effect of GO on the epoxy curing. (a) GO-catalyzed primary amine addition, (b) GO-catalyzed secondary amine addition, and (c) GO/epoxy etherification.

Table 3. Curing constants for GO/epoxy nanocomposites.

Sample	T(°C)	K_1(x10^4 s^{-1})	K_2(x10^4 s^{-1})	m	n	E_1 (kJ mol^{-1})	E_2 (kJ mol^{-1})	lnA_1	lnA_2
Epoxy	170	2.5	5.3	0.44	1.54	94.2	55.3	17.3	7.5
	175	3.6	6.5	0.46	1.51				
	180	4.4	7.3	0.43	1.47				
GO-1/ Epoxy	170	3.0	5.7	0.47	1.48	83.9	35.6	14.7	2.2
	175	4.0	6.0	0.46	1.50				
	180	5.0	7.0	0.47	1.51				
GO-2/ Epoxy	170	3.3	5.2	0.46	1.55	59.8	37.8	8.2	2.7
	175	4.3	5.8	0.43	1.44				
	180	4.7	6.5	0.40	1.48				
GO-3/ Epoxy	170	3.2	5.0	0.45	1.47	77.2	44.2	12.9	4.4
	175	3.8	6.0	0.42	1.49				
	180	5.1	6.6	0.42	1.46				

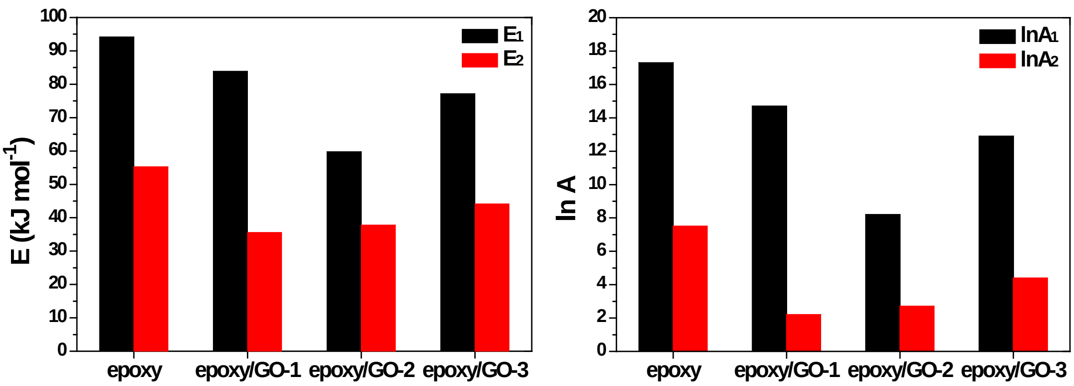

Figure 10. Activation energy and pre-exponential factor for epoxy and its nanocomposites.

To further understand the catalytic effects of the three sizes of GO on the curing behaviour of epoxy resin, activation energy, E was calculated according to Kamal's model [35] on isothermal kinetics analysis. The plots of $d\alpha/dt$ versus α were fitted by the following equation.

$$\frac{d\alpha}{dt} = (K_1+K_2\alpha^m)(1-\alpha)^n \quad (3)$$

where K_1 and K_2 are the reaction rate constants in the initial and autocatalytic stages, respectively. m and n are the reaction order of the cure. Furthermore, the temperature dependent rate constant K_i was correlated by the Arrhenius equation.

$$K_i = A\exp(-\frac{E}{RT}) \quad (4)$$

where R is the gas constant, T is the absolute temperature and A is the pre-exponential or frequency factor. The curing constants for epoxy resin and its nanocomposites were listed in Table 3. In particular, comparison of E and lnA between the epoxy with different sizes of GO are shown in figure 10. E_1 revealed the effect of GO on the epoxy resin at the initial curing stages. In contrast, E_2 was more important at the later stages, as it showed the influence of GO on the network formation in the epoxy. It can be observed that the presence of GO reduced the activation energy of the reaction, compared with the pure epoxy. The activation energy required for curing was thus declined, which demonstrated the catalytic effect of GO on the cure. Furthermore, the results revealed that E_1 decreased with the decrease of GO size from GO-1 to GO-2. Meanwhile the E_2 did not show obvious change. However, with further decreasing the GO size to that of GO-3, both of E_1 and E_2 tended to elevate. Similar variations were exhibited in lnA_1 and lnA_2.

Figure 11 shows the plots of activation energy and pre-exponential factor versus conversion, respectively. The onset activation energy of the pure epoxy resin was 94.2 kJ mol^{-1}. It decreased substantially at the initial stages of the cure, where $0<\alpha<0.2$. The reduced activation energy was benefit to the initiation rate and subsequent auto-acceleration of the cure. Accordingly, the maximal conversion rate appeared at the conversion near 0.2. At the later stages of the reaction after $\alpha = 0.2$, the decrease trend of the activation energy became slow. It maintained at a relatively steady level till the end of the cure. The incorporation of the GO reduced the activation energy of the reaction throughout the curing process. Compared with the pure resin, the average activation energy was reduced by 18.9%, 28.8% and 14.6% with addition of GO-1, GO-2 and GO-3, respectively. The GO-2 with medium size showed the biggest reduction on the activation energy, which suggested the optimal catalytic effect on the cure of epoxy resin. It should be noted that although GO induced strong catalytic effect due to its functional groups, the two-dimensional layer structure of graphene could act as space hindrance, which reduced and constrained the mobility of the reactive groups of epoxy. It was adverse to the curing catalysis and efficiency. Since the three sizes of GO had the same surface chemistry, it is believed that the observed difference in the curing behaviour results from the different hindrance effect from variable GO sizes. In this study, the GO-1 possessed large graphene layer, the size of which was about one order of magnitude bigger than that of GO-2. The presence of GO-1 in the epoxy substantially increased the diffusion distance of the reactive chains surrounding the GO sheets. The hindrance effect from individual graphene layer was significant, compared with that of GO-2. However, as the GO size further reduced to that of GO-3, there was a larger number of GO sheets dispersed in the GO-3/epoxy nanocomposite than other GO-incorporated systems at fixed filler content. The increase in the number of GO sheets induced more hindrance sites than those of GO-1 and GO-2. In addition to the hindrance effect from individual GO sheets, the massive sites could synergistically confine the movement of the reactive chains at a deeper level in larger area. It eventually resulted in higher activation energy. Therefore, GO-2 incorporated nanocomposite showed overall the least hindrance effect throughout the curing reaction. The optimal catalytic effect was obtained by showing the biggest reduction on the activation energy.

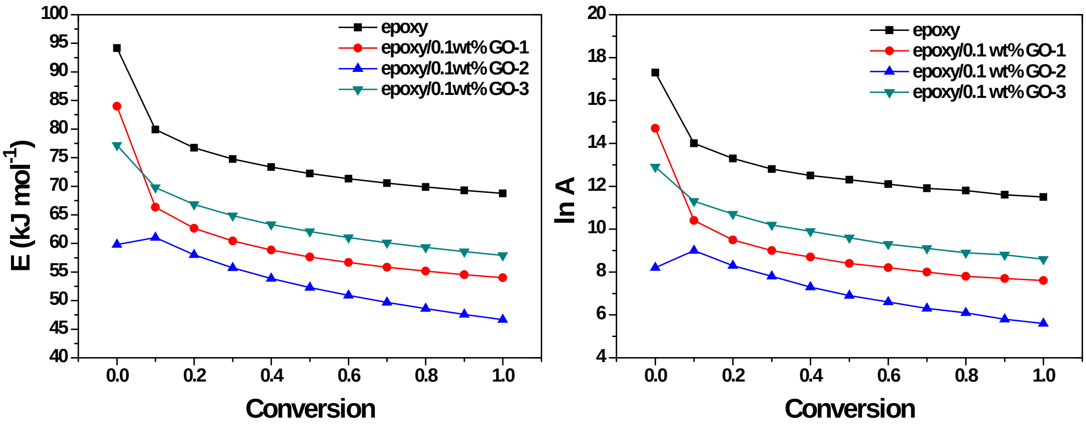

Figure 11. Activation energy and pre-exponential factor versus conversion for epoxy and its nanocomposites.

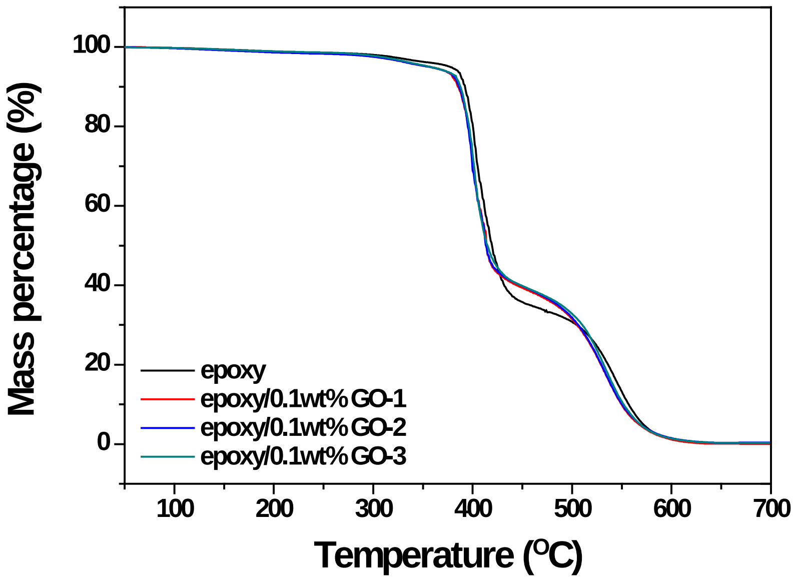

Figure 12. TGA plots of epoxy and its nanocomposites.

Table 4. Thermal properties of epoxy and its nanocomposites.

Sample	*IDT* (°C)	T_{max} (°C)	Residue (%) at 450°C
Epoxy	377	403	35.77
GO-1/epoxy	357	400	39.39
GO-2/epoxy	356	399	39.77
GO-3/epoxy	358	402	39.82

The thermal stability of the cured epoxy resin and its nanocomposites with three sizes of GO was evaluated by means of TGA. Figure 12 shows the TGA plots of the samples under air atmosphere. Table 4 lists the main indicators including initial decomposition temperature (*IDT*), temperature of the maximum rate of degradation (T_{max}) and residual weight percentage. They were used to ascertain a materials lifetime. IDT corresponded to the temperature where a 5% mass loss was accumulated. T_{max} represented the stability at main mass loss stage. It was determined at the peak of the differential Thermogravimetric curves. For the neat epoxy, it exhibited an initial decomposition at 377 °C, where unreacted and labile epoxy chains or other traces of impurities were broken [36]. The addition of GO, however reduced the *IDT* by about 20 °C. It could result from the early decomposition of the interfacial epoxy chains, the cure of which was partially inhibited by the inclusion of the two dimensional graphene layers. At the main stage of decomposition, sharp mass losses were observed in the epoxy and incorporated systems, with T_{max} at about 400 ^{o}C. The GO hardly affected the thermal behavior at this stage. As the temperature was further increased, the samples experienced a steady mass loss stage in the range of 420-500 ^{o}C. The GO/epoxy nanocomposites showed higher thermal stability than that of the pure epoxy resin at this stage. A ～4% more residue was obtained in each nanocomposite at 450^{o}C, compared with pure resin. The improved stability could be attributed to the tortuous path effect of GO [31]. The presence of GO delayed the permeation of oxygen and the escape of volatile degradation products as well as the formation of char. A notable improvement can be achieved at very low loading of 0.1 wt%, owing to the tremendous surface area of GO. Moreover, the enhancement of the thermal properties was not influenced by the variation of GO sheet size, but was determined by the loading of GO. The three sizes of GO incorporated nanocomposites showed similar degradation behavior.

4. Conclusions

The incorporation of 0.1 wt% GO catalyzed the curing reaction of epoxy resin. The activation energy was reduced by 18.9%, 28.8% and 14.6% with addition of GO-1, GO-2 and GO-3, respectively. GO-2 with medium size (1.72μm) showed the optimal catalytic effect on the cure. It resulted from the minimal hindrance that confined the mobility of reactive groups. The GO also improved the thermal stability of epoxy resin in the range of 420-500 ^{o}C. A ～4% more residue was obtained in each of the incorporated system, compared with the pure resin. However, the variations of GO sheet size did not influence the enhancement effect on the thermal stability.

Acknowledgments

This work was funded by the National Natural Science Foundation of China (NSFC) (Grant No. 51503205), Chinese Academy of Sciences (CAS) 'Light of West China' Program.

References

[1] Ratna D 2009 *Handbook of thermoset resins* (Shropshire: iSmithers)

[2] Barua S, Chattopadhyay P, Phukan M M, Konwar B K and Karak N 2014 Hyperbranched epoxy/MWCNT-CuO-nystatin nanocomposite as a high performance, biocompatible, antimicrobial material *Mater. Res. Express* **1 045402**

[3] Bedsole R W, Park C, Bogert P B and Tippur H V 2015 A critical evaluation of the enhancement of mechanical properties of epoxy modified using CNTs *Mater. Res. Express* **2 095020**

[4] Bindu Sharmila T K, Antony J V, Jayakrishnan M P, Sabura Beegum P M and Thachil E T 2016 Mechanical, thermal and dielectric properties of hybrid composites of epoxy and reduced graphene oxide/iron oxide *Mater. Des.* **90 66–75**

[5] Liu S, Fan X and He C 2016 Improving the fracture toughness of epoxy with nanosilica-rubber core-shell nanoparticles *Compos. Sci. Technol.* **125 132–40**

[6] Trihotri M, Dwivedi U K, Khan F H, Malik M M and Qureshi M S 2015 Effect of curing on activation energy and dielectric properties of carbon black–epoxy composites at different temperatures *J. Non. Cryst. Solids* **421 1–13**

[7] Wang X, Jin J and Song M 2012 Cyanate ester resin/graphene nanocomposite: curing dynamics and network formation *Eur. Polym. J.* **48 1034–41**

[8] Hu J, Shan J, Zhao J and Tong Z 2015 Water resistance and curing kinetics of epoxy resins with a novel curing agent of biphenyl-containing amine synthesized by one-pot method *Thermochim. Acta* **606 58–65**

[9] Wan J, Gan B, Li C, Molina-Aldareguia J, Kalali E N, Wang X and Wang D-Y 2016 A sustainable, eugenol-derived epoxy resin with high biobased content, modulus, hardness and low flammability: Synthesis, curing kinetics and structure–property relationship *Chem. Eng. J.* **284 1080–93**

[10] Sánchez-Cabezudo M, Prolongo M G, Salom C and Masegosa R M 2006 Cure kinetics of epoxy resin and thermoplastic polymer *J. Therm. Anal. Calorim.* **86 699–705**

[11] White S R, Mather P T and Smith M J 2002 Characterization of the cure-state of

DGEBA-DDS epoxy using ultrasonic, dynamic mechanical, and thermal probes *Polym. Eng. Sci.* **42 51–67**

[12] Zhang Z, Liang G, Ren P and Wang J 2008 Curing behavior of epoxy / POSS / DDS hybrid systems *Polym. Compos.* **51 1–7**

[13] Arabli V and Aghili A 2013 Effect of silica nanoparticles on the curing kinetics of epoxy vinyl ester resin *Proc. Int. Conf. Nanomater. Appl. Prop.* **2 03NCNN26**

[14] Ferdosian F, Ebrahimi M and Jannesari A 2013 Curing kinetics of solid epoxy/DDM/nanoclay: Isoconversional models versus fitting model *Thermochim. Acta* **568 67–73**

[15] Zhou T, Wang X, Liu X and Xiong D 2009 Influence of multi-walled carbon nanotubes on the cure behavior of epoxy-imidazole system *Carbon* 47 **1112–8**

[16] Zheng X, Li D, Feng C and Chen X 2015 Thermal properties and non-isothermal curing kinetics of carbon nanotubes/ionic liquid/epoxy resin systems *Thermochim. Acta* **618 18–25**

[17] Zhou T, Wang X, Liu X H and Lai J Z 2010 Effect of silane treatment of carboxylic-functionalized multi-walled carbon nanotubes on the thermal properties of epoxy nanocomposites *eXPRESS Polym. Lett.* **4 217–26**

[18] Zhou T, Wang X and Wang T 2009 Cure reaction of multi-walled carbon nanotubes/diglycidyl ether of bisphenol A/2-ethyl-4-methylimidazole (MWCNTs/DGEBA/EMI-2,4) nanocomposites: effect of carboxylic functionalization of MWCNTs *Polym. Int.* **58 445–52**

[19] Li A, Li W, Ling Y, Gan W, Brady M A and Wang C 2016 Effects of silica-coated carbon nanotubes on the curing behavior and properties of epoxy composites *RSC Adv*. **6 23318–26**

[20] Xie H, Liu B, Sun Q, Yuan Z, Shen J and Cheng R 2005 Cure kinetic study of carbon nanofibers/epoxy composites by isothermal DSC *J. Appl. Polym. Sci.* **96 329–35**

[21] Vertuccio L, Russo S, Raimondo M, Lafdi K and Guadagno L 2015 Influence of carbon nanofillers on the curing kinetics of epoxy-amine resin *RSC Adv.* **5 90437–50**

[22] Abdalla M, Dean D, Robinson P and Nyairo E 2008 Cure behavior of epoxy/MWCNT nanocomposites: The effect of nanotube surface modification *Polymer* **49 3310–7**

[23] Jana S and Zhong W-H (Katie) 2009 Curing characteristics of an epoxy resin in the presence of ball-milled graphite particles *J. Mater. Sci.* **44 1987–97**

[24] Guo B, Wan J, Lei Y and Jia D 2009 Curing behaviour of epoxy resin/graphite composites containing ionic liquid *J. Phys. D Appl. Phys.* **42 145307**

[25] Wang X, Jin J and Song M 2013 An investigation of the mechanism of graphene toughening epoxy *Carbon* **65 324–33**

[26] Wang X and Song M 2013 Toughening of polymers by graphene *Nanomater. Energy* **2 1–37**

[27] Wang F, Drzal L T, Qin Y and Huang Z 2016 Size effect of graphene nanoplatelets on the morphology and mechanical behavior of glass fiber/epoxy composites *J. Mater. Sci.* **51 3337–48**

[28] Qiu S L, Wang C S, Wang Y T, Liu C G, Chen X Y, Xie H F, Huang Y A and Cheng R S 2011 Effects of graphene oxides on the cure behaviors of a tetrafunctional epoxy resin *Express Polym. Lett.* **5 809–18**

[29] Ryu S H, Sin J H and Shanmugharaj A M 2014 Study on the effect of hexamethylene diamine functionalized graphene oxide on the curing kinetics of epoxy nanocomposites *Eur. Polym. J.* **52 88–97**

[30] Li L, Zeng Z, Zou H and Liang M 2015 Curing characteristics of an epoxy resin in the presence of functional graphite oxide with amine-rich surface *Thermochim. Acta* **614 76–84**

[31] Wang X, Xing W, Zhang P, Song L, Yang H and Hu Y 2012 Covalent functionalization of graphene with organosilane and its use as a reinforcement in epoxy composites *Compos. Sci. Technol.* **72 737–43**

[32] Wan Y J, Yang W H, Yu S H, Sun R, Wong C P and Liao W H 2016 Covalent polymer functionalization of graphene for improved dielectric properties and thermal stability of epoxy composites *Compos. Sci. Technol.* **122 27–35**

[33] Liu S, Yan H, Fang Z and Wang H 2014 Effect of graphene nanosheets on morphology, thermal stability and flame retardancy of epoxy resin *Compos. Sci. Technol.* **90 40–7**

[34] Hummers W S and Offeman R E 1958 Preparation of graphitic oxide *J. Am. Chem. Soc.* **80(6) 1339**

[35] Kamal M R 1974 Thermoset characterization for moldability analysis *Polym. Eng. Sci.* **14 231–9**

[36] Thomas R, Yumei D, Yuelong H, Le Y, Moldenaers P, Weimin Y, Czigany T and Thomas S 2008 Miscibility, morphology, thermal, and mechanical properties of a DGEBA based epoxy resin toughened with a liquid rubber *Polymer* **49 278–94**